1 Experimental

All chemicals were used as purchased from Fisher Scientific, Sigma-Aldrich and Alfa Aesar unless otherwise stated. NMR spectra were recorded on a Bruker DPX300 NMR spectrometer with shifts referenced to the residual solvent signal. Mass spectra were recorded on a Bruker microTOF mass spectrometer using electrospray ionization. FTIR spectra were recorded on a Thermo Nicolet 380 spectrometer using KBr pellets. Powder X-ray diffraction data was recorded on a PANalytical X'Pert Pro MPD in Bragg-Brentano geometry, with monochromated Cu $K_{\alpha 1}$ ($\lambda = 1.5406$ Å, 40 kV, 40 mA) radiation, automated divergence and receiving slits (10 mm illuminated length), 10 mm beam mask, 0.04 rad soller slits and a step size of 0.08°. UV-Vis spectra were recorded on a Perkin-Elmer Lambda 25 spectrometer using quartz cells with a 1 cm path length.

Atomic Force Microscopy (AFM) images were acquired on an Asylum Research MFP-3D microscope using tapping mode, with a scan rate of 0.4 Hz. Igor Pro software was used for image acquisition and images were presented as amplitude traces. AFM samples were prepared from 0.001 wt % suspensions dried on mica sheets.

X-ray Photoelectron Spectra were recorded on a Kratos Axis Ultra X-ray Photoelectron Spectrometer employing a monochromated Al K_{α} ($h\nu = 1486.6$ eV, 120 W) X-ray source, hybrid (magnetic/electrostatic) optics (300 x 700 µm aperture), hemispherical analyser, multichannel plate and delay line detector (DLD) with a take-off angle of 90° and an acceptance angle of 30°. All scans were acquired under charge neutralization conditions using a low energy electron gun within the field of the magnetic lens. Survey scans were taken with a pass energy of 80 eV and high resolution scans with a pass energy of 20 eV.

1.1 Cotton hydrolysis

Sulfuric acid (400 ml, 64 %) was heated at 45 °C and cotton wool (47.1 g) added slowly with mechanical stirring. Stirring and heating was continued for 35 minutes before addition of deionized water to quench the reaction. The cellulose was separated from the acidic reaction media by centrifugation (10,000 rpm, 10 °C)

for 20 minutes. The solid product was washed with two successive centrifugations (10,000 rpm, 10 °C) for 35 minutes, before dialysing against water for 48 hours. The nanocrystal suspension was homogenized using a sonifier before filtration to separate aggregates. The resulting homogeneous suspension was mixed with Amberlite MB 6113 mixed bed ion exchange resin (100 g) for 12 hours, frozen in liquid nitrogen, then freeze dried. The cellulose nanocrystals were subsequently soxhlet extracted with ethanol (48 hours) to remove organic surface contaminants and dried *in vacuo*. Found (%): C, 42.6; H, 6.05.

1.2 Synthesis of 6-chlorodeoxycellulose nanocrystals

Cellulose nanocrystals (2 g) were suspended in a solution of pyridine (20 ml, 250 mmol) and dry toluene (400 ml) under argon. A solution of thionyl chloride (25 ml, 135 mmol) in dry toluene (100 ml) was added dropwise before subsequent heating at 65 °C for 16 hours. The resulting light brown suspension was filtered and the product washed with dichloromethane (20 ml), deionized water (50 ml) and acetone (20 ml) before soxhlet extraction with dichloromethane (24 hours) and ethanol (48 hours). The light brown chlorinated nanocrystals were isolated by drying *in vacuo*. IR (KBr): $\tilde{\nu} = 715\,\mathrm{cm}^{-1}$. Found (%): C, 36.1; H, 5.70; Cl, 8.00.

1.3 Synthesis of 6-azidodeoxycellulose nanocrystals

6-Chlorodeoxycellulose nanocrystals (270 mg) were suspended in dimethylformamide (20 ml) with sodium azide (680 mg, 39 mmol) and heated at 100 °C for 2 days. The solid product was separated by filtration and washed with deionized water (4 x 50 ml) and ethanol (2 x 20 ml) before dispersing in deionized water and dialysis against deionized water for 2 days. The product was subsequently isolated by freeze drying. IR (KBr): $\tilde{\nu} = 2114\,\mathrm{cm}^{-1}$. Found (%): C, 40.95; H, 5.5; N, 3.66.

1.4 Synthesis of 3-methyl-1-propargylimidazolium bromide ([MPIM][Br])

Methylimidazole (10 ml, 125 mmol) was added dropwise to an 80 % solution of propargyl bromide (16.97 g, 143 mmol) in toluene (15.37 ml) at −10 °C under argon. The reaction was allowed to warm to room temperature slowly, and dry toluene (50 ml) was added before leaving the brown suspension to stir overnight. The solvent was removed *in vacuo* to yield a pale brown product. IR (ATR): $\tilde{\nu} = 2122, 1566, 1164, 745\,\mathrm{cm}^{-1}$. ^{1}H NMR (300 MHz, DMSO-d_6): $\delta = 3.86$ (t, $J = 2.5$ Hz, 1H, HC≡C), 3.88 (s, 3H, CH_3), 5.23 (d, $J = 2.5$ Hz, 2H, CH_2), $7.76 - 7.79$ (m, 1H, ImH), $7.80 - 7.83$ (m, 1H, ImH), $9.24 - 9.30$ (m, 1H, ImH) ppm. ^{13}C NMR (75 MHz, DMSO-d_6): $\delta = 36.0, 38.5, 76.1, 78.9, 122.1, 124.0, 136.6$ ppm. m/z (ESI): 121.08 $(M)^+$, 321.07 $(2M+Br)^+$.

1.5 Synthesis of 3-methyl-1-((1-(6-deoxycellulos-6-yl)-1,2,3-triazol-4-yl)methyl)imidazolium bromide ([MPIM]-g-cellulose nanocrystals)

6-Azidodeoxycellulose nanocrystals (200 mg) and 3-methyl-1-propargylimidazolium bromide (80 mg, 0.4 mmol) were suspended in deionized water (20 ml) and 0.1 M copper(II) sulfate (1 ml, 0.1 mmol) and 0.1 M sodium ascorbate (3 ml, 0.3 mmol) were added before heating the suspension at 70 °C for 2 days. The solid product was isolated by centrifugation, then washed by 2 successive centrifugations with deionized water before dialysing against deionized water for 5 days and isolation by freeze drying. Found (%): C, 42.36; H, 5.58; N, 3.40.

1.6 Synthesis of 3-methyl-1-((1-(6-deoxycellulos-6-yl)-1,2,3-triazol-4-yl)methyl)imidazolium bis(trifluoromethanesulfonyl)imide ([MPIM][NTf_2]-g-cellulose nanocrystals)

3-Methyl-1-((1-(6-deoxycellulos-6-yl)-1,2,3-triazol-4-yl)methyl)imidazolium bromide (50 mg) and lithium bis-(trifluoromethanesulfonyl)imide (30 mg, 0.1 mmol) were suspended in deionized water (5 ml) and stirred for 24

hours before isolation and washing by 10 successive centrifugations with deionized water and freeze drying.

2 Calculation of degree of substitution

Using the dimensions of the long ($L = 14\,\text{nm}$) and short ($l = 7.3\,\text{nm}$) sides of the nanocrystal cross section,[1] and considering that the ($\mathbf{1\bar{1}0}$) planes ($d = 0.62\,\text{nm}$) are parallel to the long side, and the ($\mathbf{110}$) planes ($d = 0.53\,\text{nm}$) parallel to the short side, the ratio of chains accessible at the surface can be calculated using the method by Habibi *et al.*[2]

$$\begin{aligned}\frac{\text{Surface Chains}}{\text{Total Chains}} &= \frac{\left(\frac{2L}{d_{(110)}}\right) + \left(\frac{2l}{d_{(1\bar{1}0)}}\right)}{\left(\frac{Ll}{d_{(1\bar{1}0)}d_{(110)}}\right)} \\ &= \frac{\left(\frac{2\times 14}{0.532}\right) + \left(\frac{2\times 7.3}{0.588}\right)}{\left(\frac{14\times 7.3}{0.588\times 0.532}\right)} \\ &= 0.24\end{aligned}$$

Using the ratio for surface chains to internal chains, the empirical formulae for the anhydroglucose units in the modified samples were determined assuming a surface degree of substitution of 1, along with the associated expected atomic and weight percentage compositions. The degree of substitution by elemental analysis was then calculated by an iterative method. The differences in carbon and hydrogen values with respect to the calculated values remain constant between each modification reaction and are present in unmodified cellulose.

3 Infrared Spectra

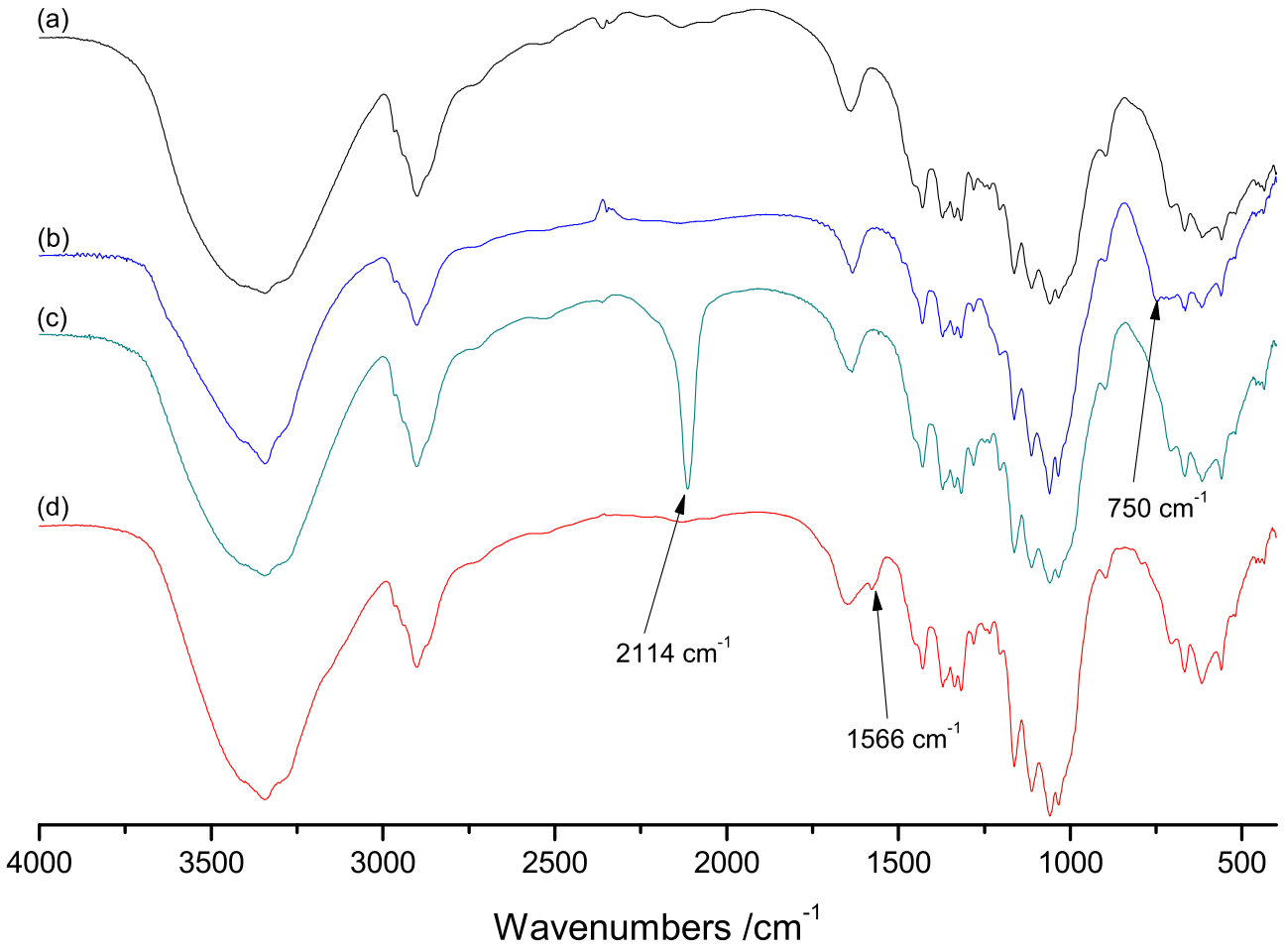

Figure 1 Transmission FTIR spectra showing modification of CNXLs: (a) CNXLs; (b) Chlorinated CNXLs; (c) Azidated CNXLs; (d) [MPIM][Br] grafted CNXLs.

4 Powder X-ray Diffraction Data

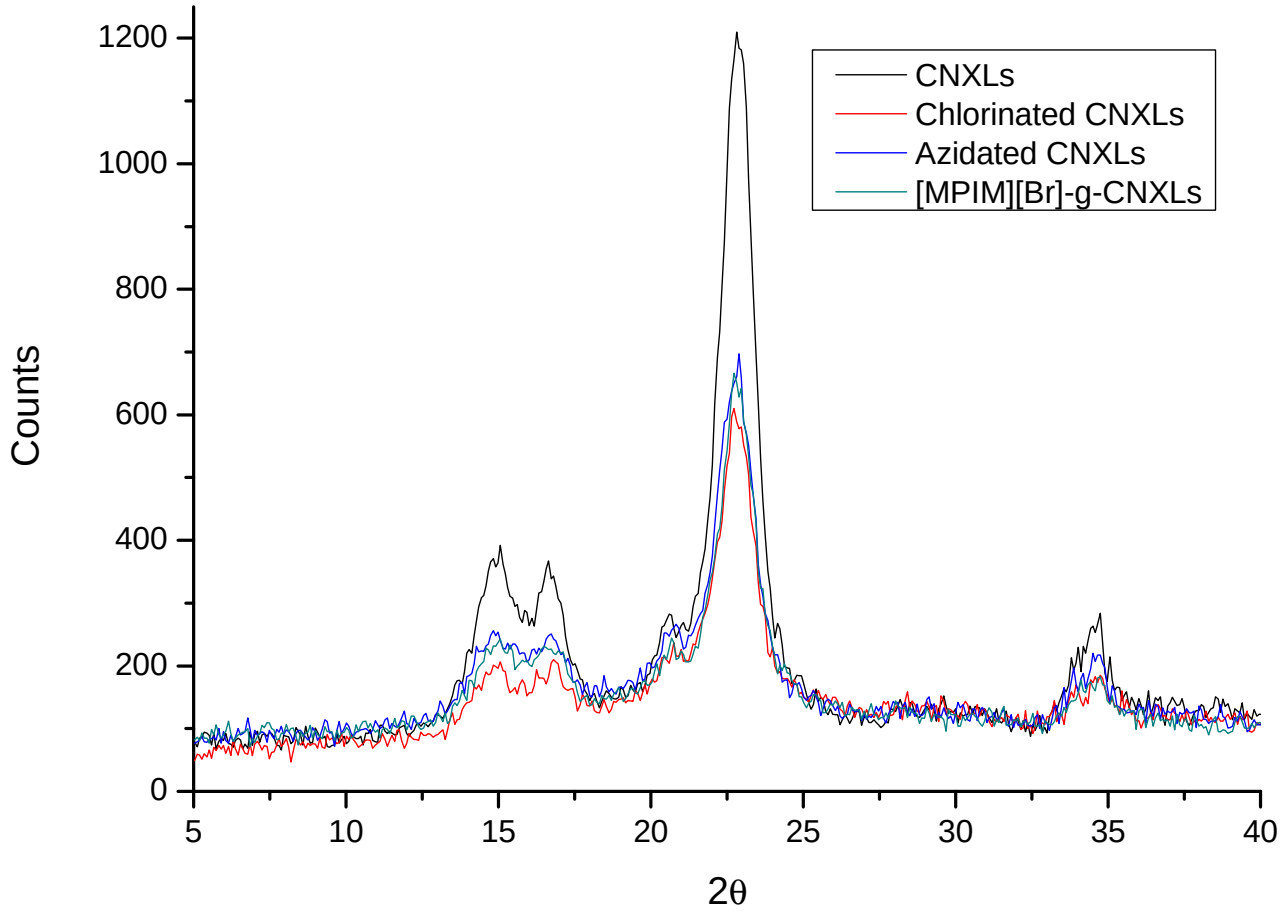

Figure 2 Diffractograms for Cellulose Nanocrystal Derivatives

The d-spacing of the $(\mathbf{1\bar{1}0})$ and $(\mathbf{110})$ planes were calculated from the XRD data for cellulose nanocrystals ($2\theta = 15.07$ and $2\theta = 16.65$ respectively).

$$\begin{aligned} d_{(\mathbf{1\bar{1}0})} &= \frac{\lambda}{2\sin\theta} \\ &= \frac{1.5405980}{2\sin 7.5336955} \\ &= 5.875\text{Å} \end{aligned}$$

$$\begin{aligned} d_{(\mathbf{110})} &= \frac{\lambda}{2\sin\theta} \\ &= \frac{1.5405980}{2\sin 8.3236955} \\ &= 5.321\text{Å} \end{aligned}$$

The crystallinity indices were calculated for each sample using Equation 3,[3] and are shown in Table 1

$$\chi_c = \frac{I_{(\mathbf{200})} - I_a}{I_{(\mathbf{200})}}$$

Figure 3 Equation for the crystallinity index, where $I_{(\mathbf{200})}$ is the intensity of the (200) peak, and I_a is the intensity of the amorphous background around $2\theta = 18°$.

Table 1 Crystallinity Indices

Compound	$I_{(\mathbf{200})}$	I_a	χ_c
Cellulose Nanocrystals	1210	133	0.89
Chlorinated Cellulose Nanocrystals	610	125	0.80
Azidodeoxycellulose Nanocrystals	697	157	0.78
MPIM-g-cellulose Nanocrystals	734	213	0.79

5 X-ray Photoelectron Spectroscopy

Table 2 Cellulose Nanocrystals XPS Data

Element	**Orbital**	**Binding Energy /eV**	**At %**
Carbon	1s	286.6	59.5
Oxygen	1s	532.6	40.5

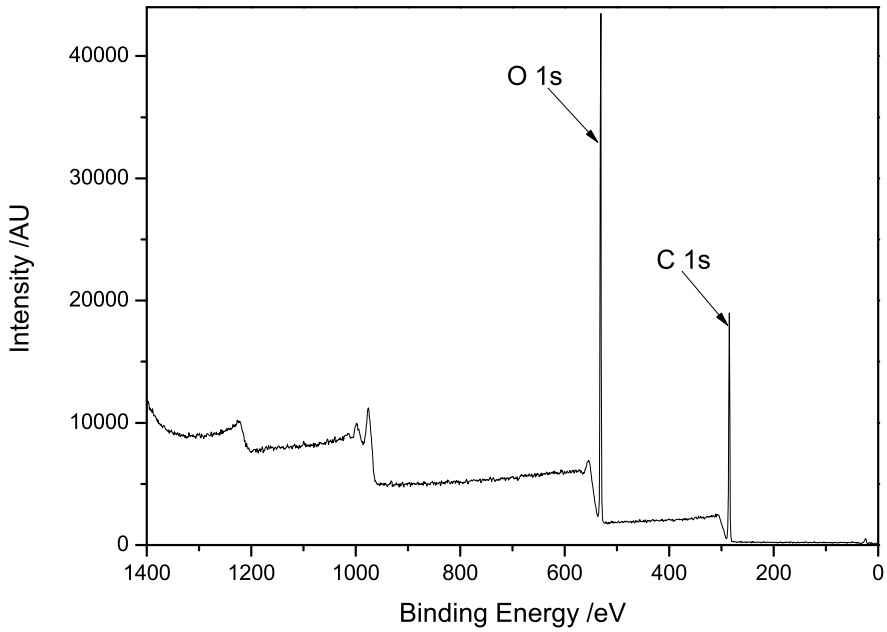

Figure 4 XPS Wide Scan of Cellulose Nanocrystals

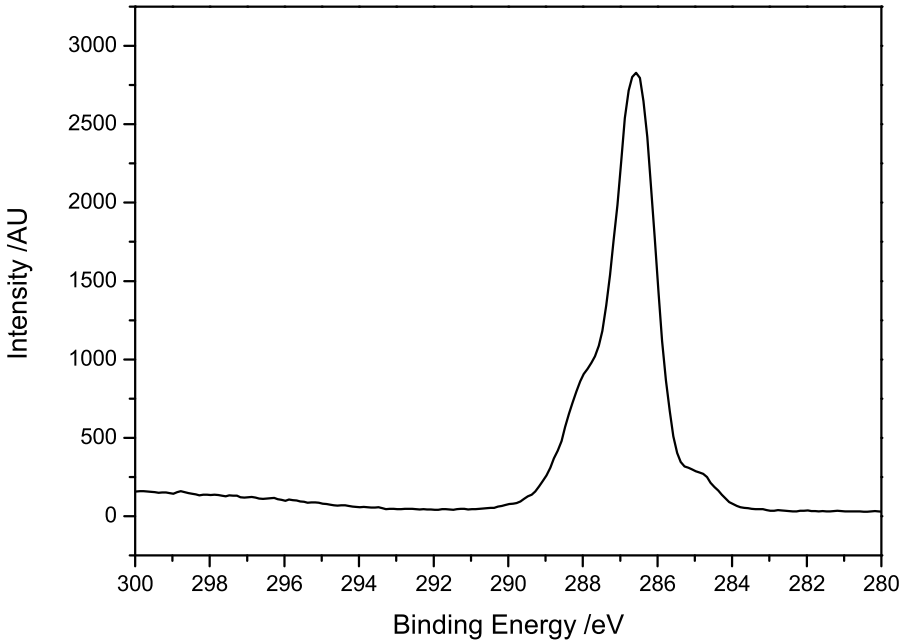

Figure 5 XPS High Resolution Carbon 1s Scan of Cellulose Nanocrystals

Table 3 Chlorodeoxycellulose Nanocrystals XPS Data

Element	Orbital	Binding Energy /eV	At %
Carbon	1s	286.9	59.6
Oxygen	1s	533.3	31.7
Chlorine	2p	200.7	8.7

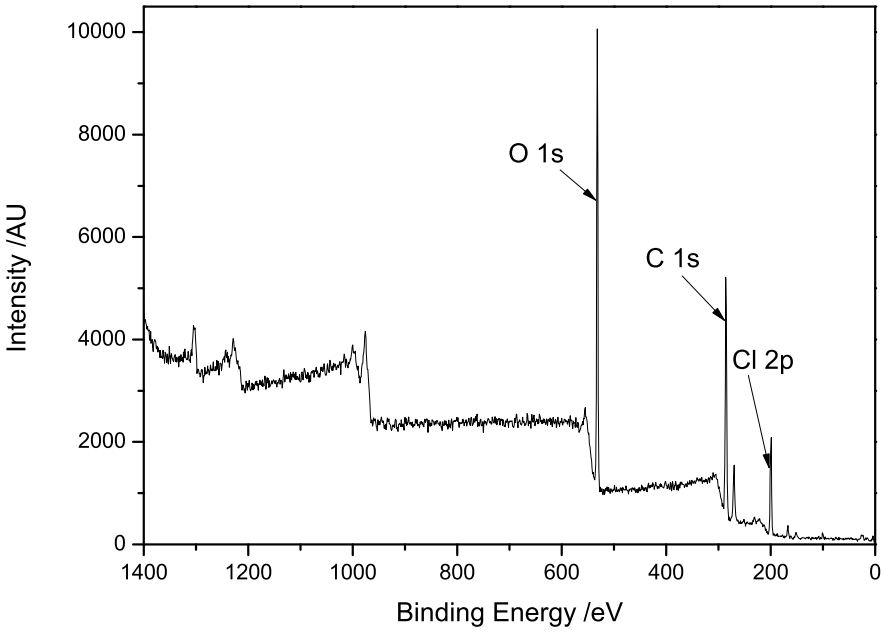

Figure 6 XPS Wide Scan of Chlorodeoxycellulose Nanocrystals

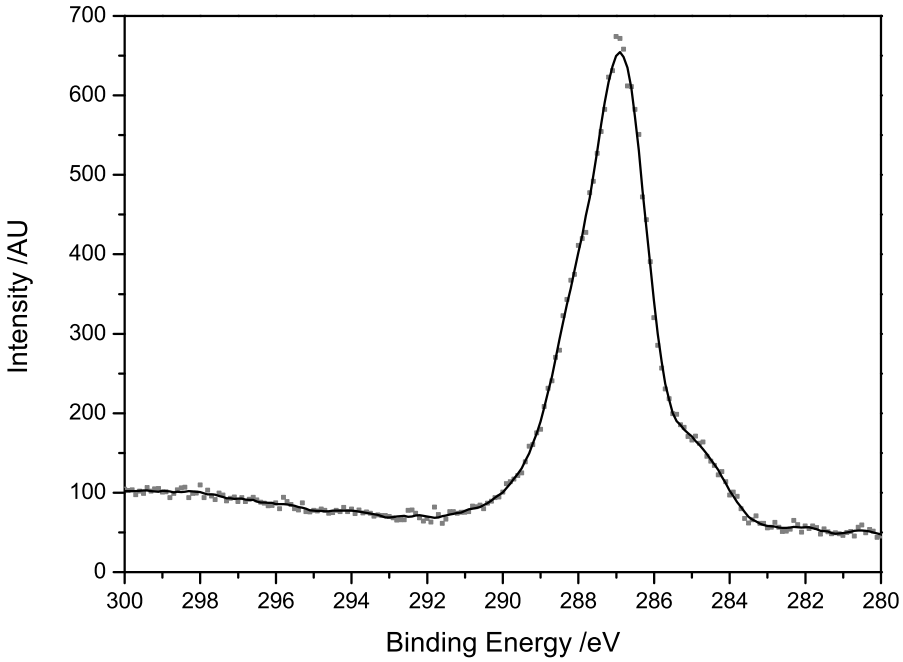

Figure 7 XPS High Resolution Carbon 1s Scan of Chlorodeoxycellulose Nanocrystals

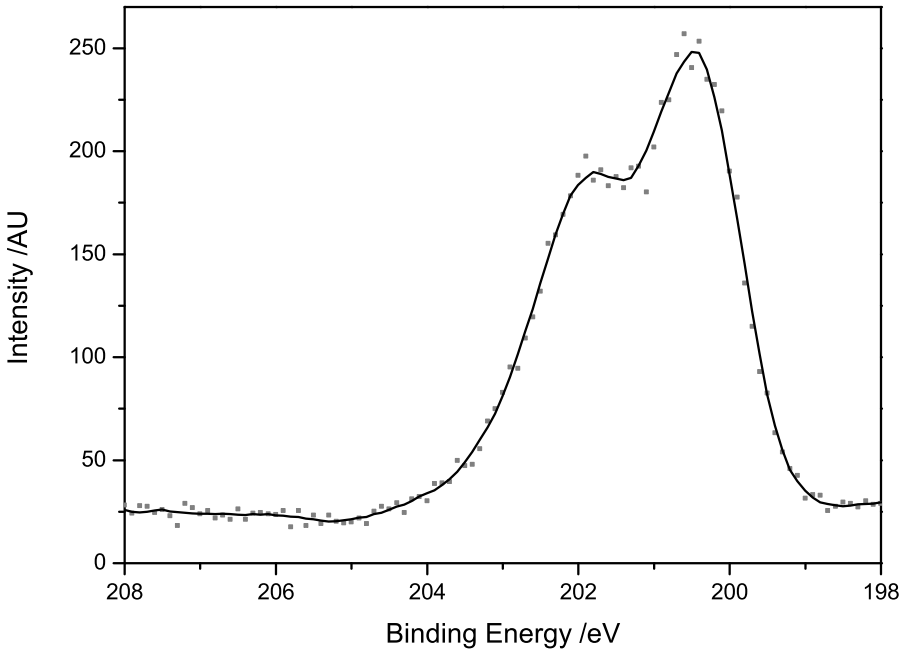

Figure 8 XPS High Resolution Chlorine 2p Scan of Chlorodeoxycellulose Nanocrystals

Table 4 Azidodeoxycellulose Nanocrystals XPS Data

Element	**Orbital**	**Binding Energy /eV**	**At %**
Carbon	1s	286.6	53.9
Oxygen	1s	532.9	41.8
Nitrogen	1s	404.6 & 400.8	4.3

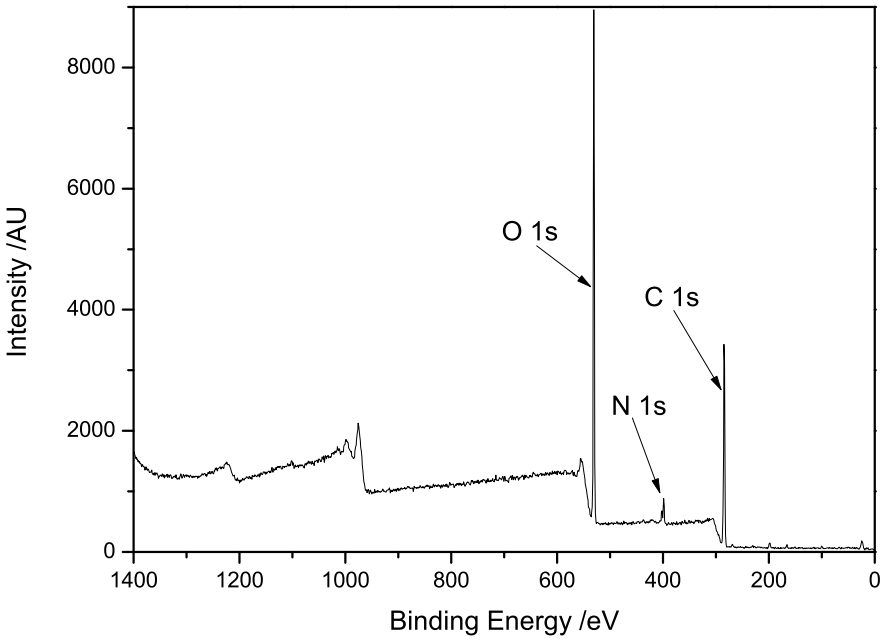

Figure 9 XPS Wide Scan of Azidodeoxycellulose Nanocrystals

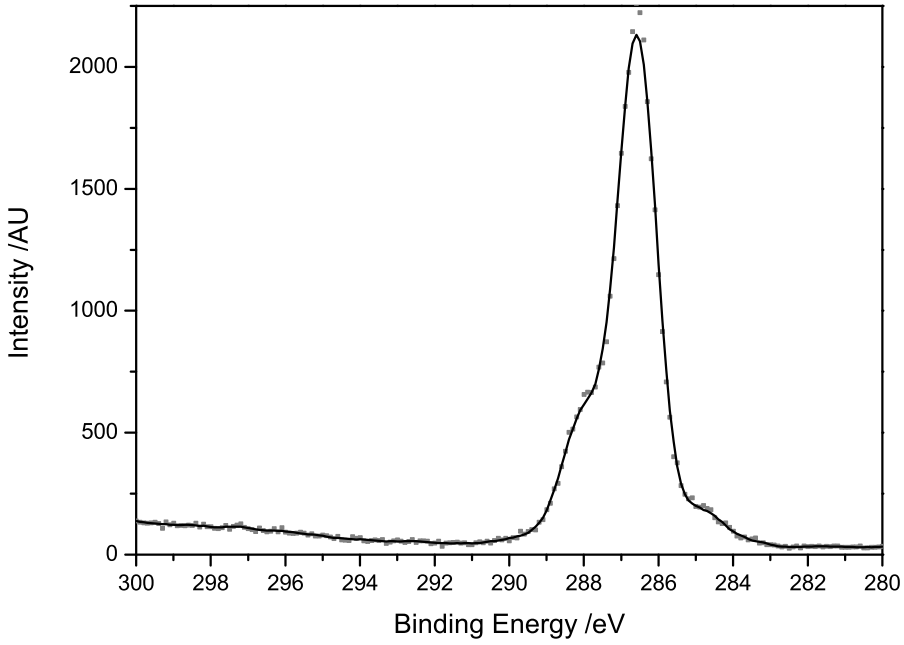

Figure 10 XPS High Resolution Carbon 1s Scan of Azidodeoxycellulose Nanocrystals

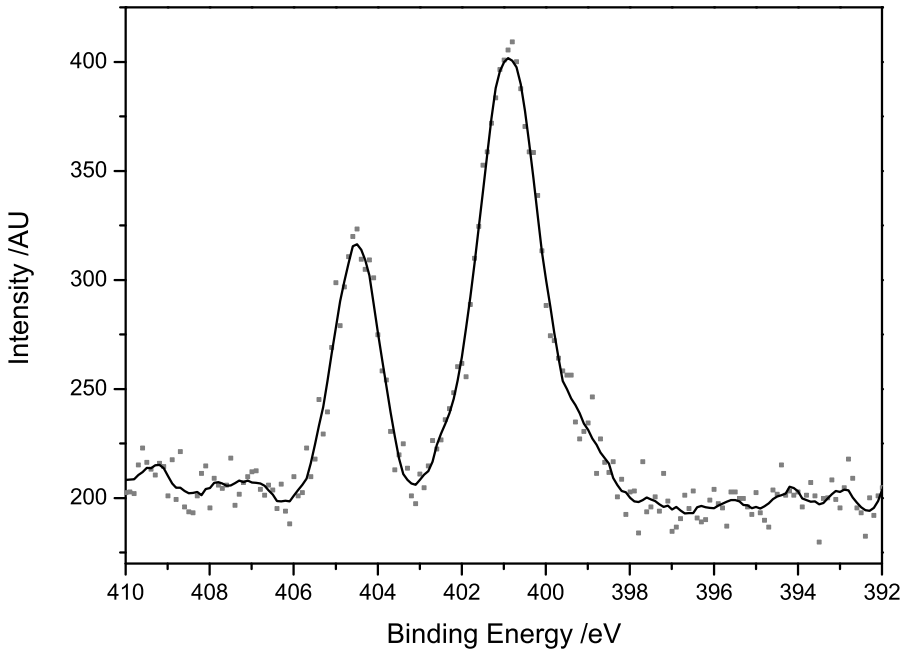

Figure 11 XPS High Resolution Nitrogen 1s Scan of Azidodeoxycellulose Nanocrystals

Table 5 MPIM-g-cellulose Nanocrystals XPS Data

Element	Orbital	Binding Energy /eV	At %
Carbon	1s	286.5	62.6
Oxygen	1s	532.8	33.0
Nitrogen	1s	401.8 & 400.5	4.4

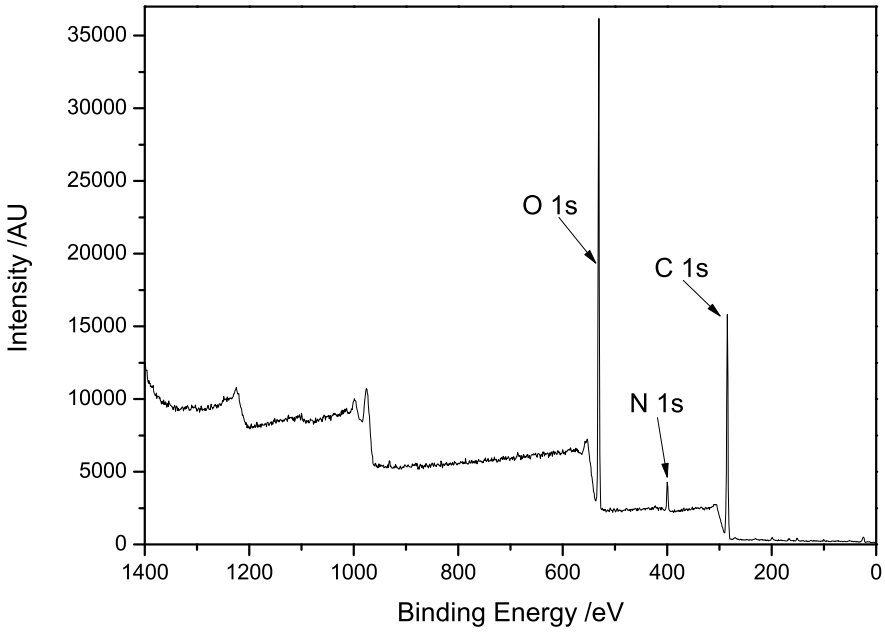

Figure 12 XPS Wide Scan of MPIM-g-cellulose Nanocrystals

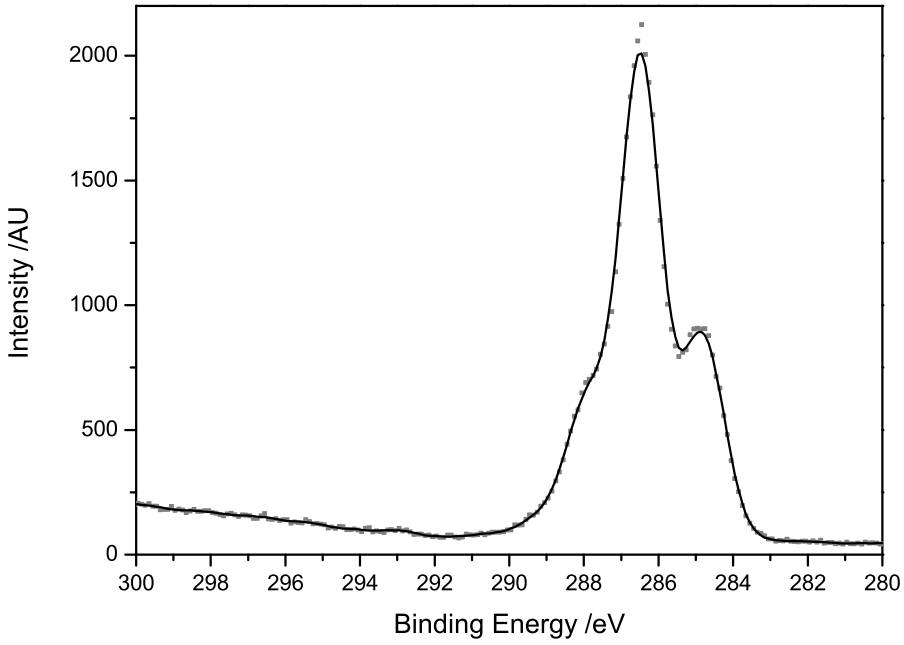

Figure 13 XPS High Resolution Carbon 1s Scan of MPIM-g-cellulose Nanocrystals

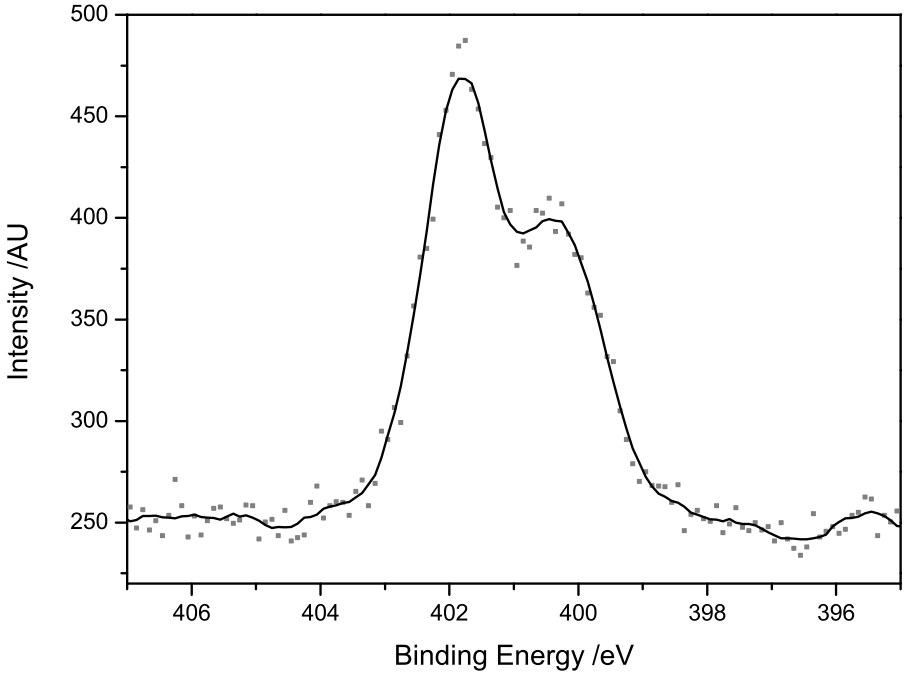

Figure 14 XPS High Resolution Nitrogen 1s Scan of MPIM-g-cellulose Nanocrystals

Table 6 [NTf2][MPIM]-g-cellulose Nanocrystals XPS Data

Element	Orbital	Binding Energy /eV	At %
Carbon	1s	286.6 & 293.0	53.2
Oxygen	1s	533.0	35.7
Nitrogen	1s	401.9 & 400.3	4.1
Sulfur	2p	169.1	1.0
Fluorine	1s	688.9	5.9

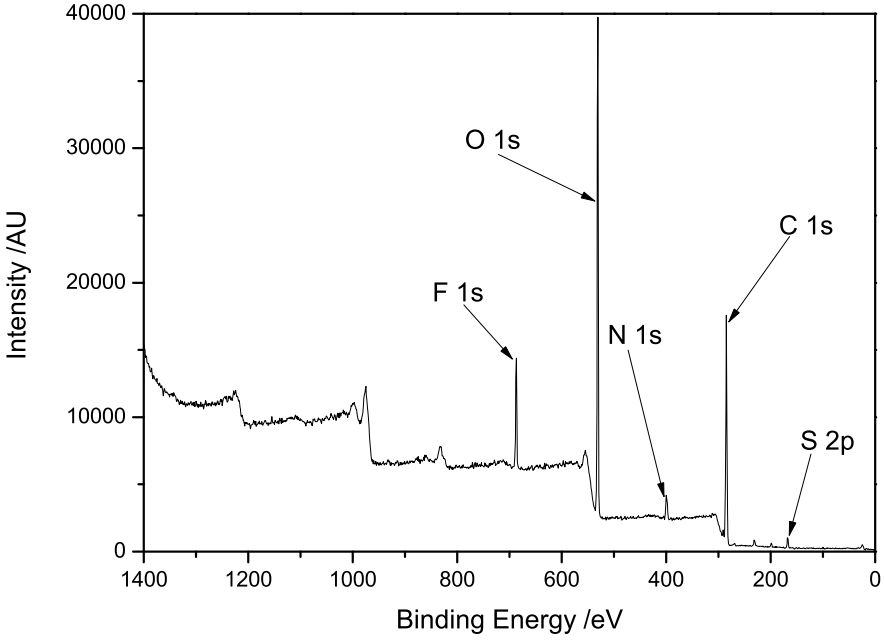

Figure 15 XPS Wide Scan of [NTf2][MPIM]-g-cellulose Nanocrystals

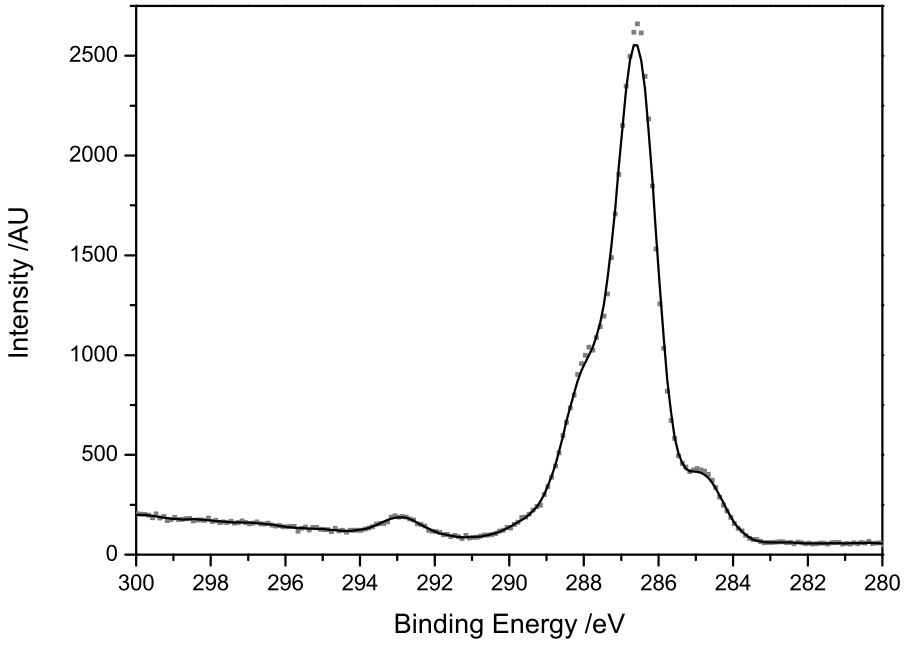

Figure 16 XPS High Resolution Carbon 1s Scan of [NTf2][MPIM]-g-cellulose Nanocrystals

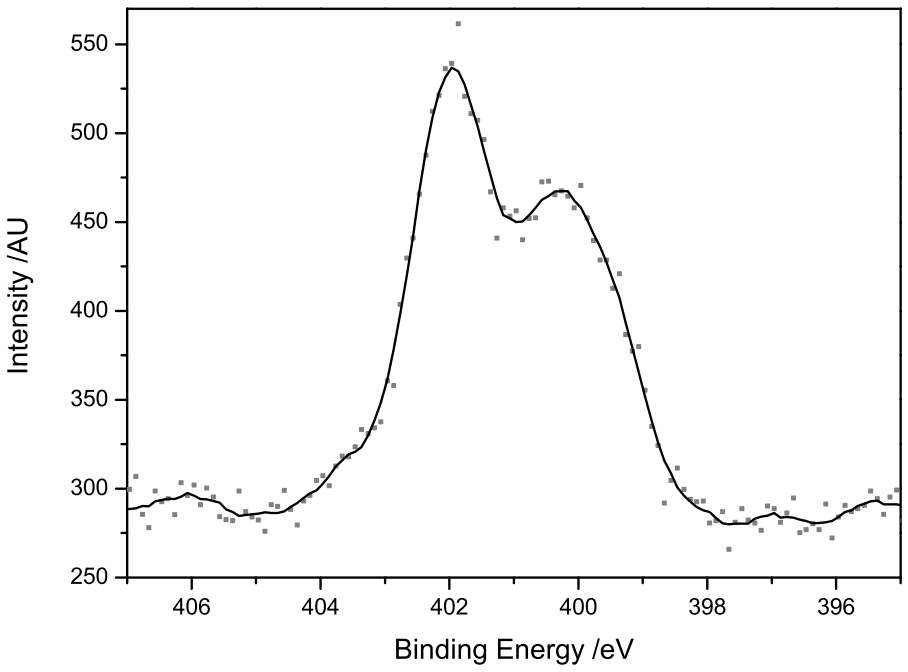

Figure 17 XPS High Resolution Nitrogen 1s Scan of [NTf2][MPIM]-g-cellulose Nanocrystals

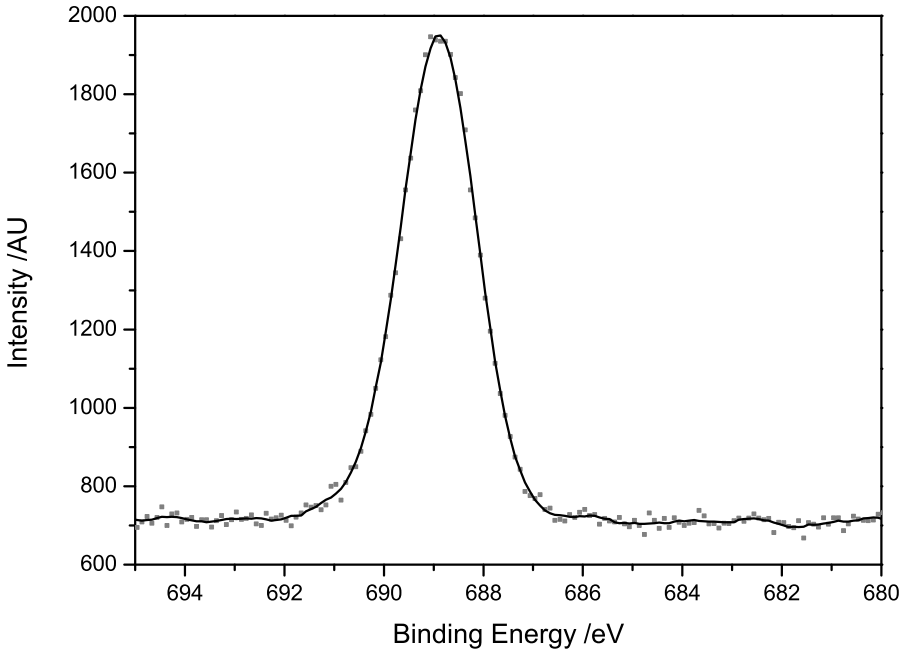

Figure 18 XPS High Resolution Fluorine 1s Scan of [NTf2][MPIM]-g-cellulose Nanocrystals

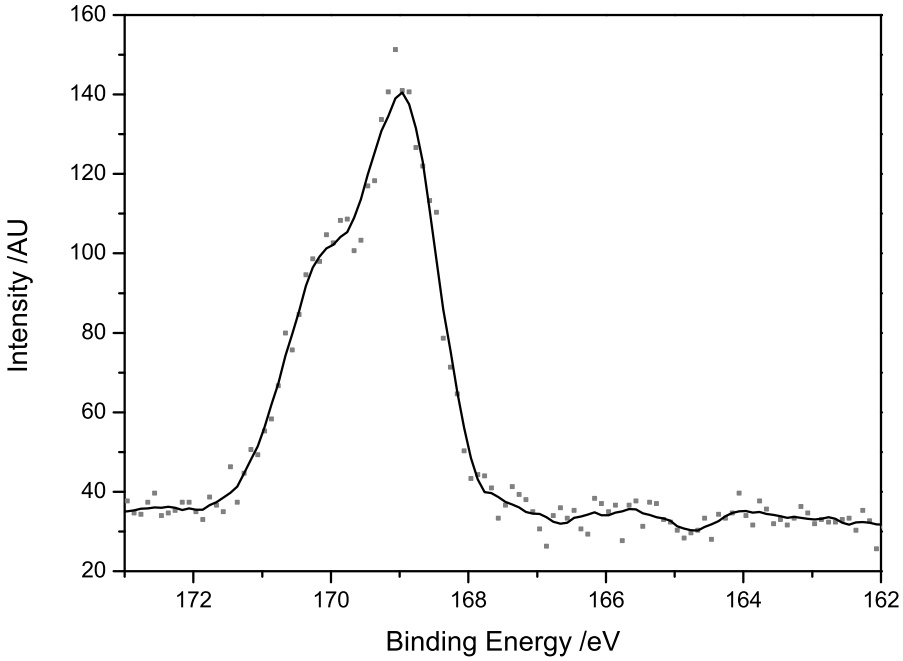

Figure 19 XPS High Resolution Sulfur 2p Scan of [NTf2][MPIM]-g-cellulose Nanocrystals

6 AFM Image of [Br][MPIM]-g-CNXLs

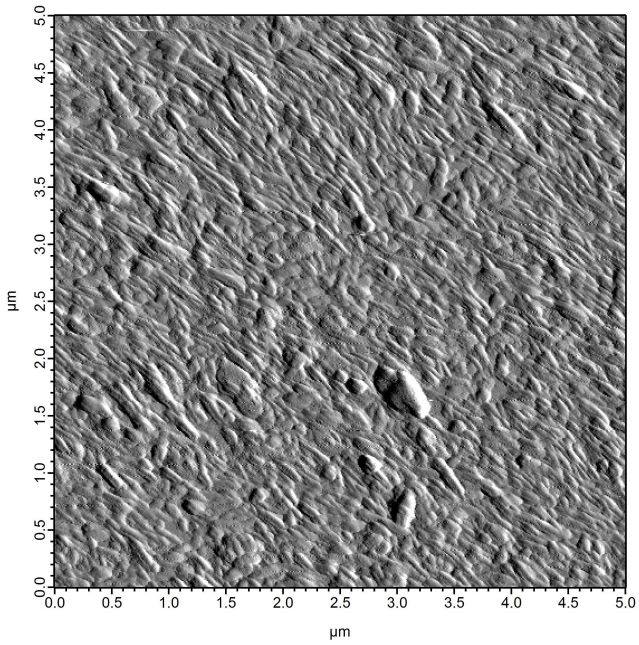

Figure 20 AFM image of [Br][MPIM]-g-CNXLs showing aggregation on the mica surface

References

[1] Elazzouzi-Hafraoui, S.; Nishiyama, Y.; Putaux, J.; Heux, L.; Dubreuil, F.; Rochas, C. *Biomacromolecules* **2008**, *9*, 57–65.

[2] Habibi, Y.; Chanzy, H.; Vignon, M. R. *Cellulose* **2006**, *13*, 679–687.

[3] Cao, Y.; Tan, H. *Enzyme Microb. Technol.* **2005**, *36*, 314–317.